The Structure of NO_3^- in Molten Monovalent Metal Nitrates by Pulsed Neutron Diffraction

Kenji Suzuki and Yoshiaki Fukushima

The Research Institute for Iron, Steel and Other Metals, Tohoku University, Sendai-980, Japan

(Z. Naturforsch. **32 a**, 1438–1443 [1977]; received June 3, 1977)

The structure factor of molten monovalent metal nitrates was measured over a wide range of scattering vectors by time-of-flight pulsed neutron diffraction using epithermal neutrons generated from an electron LINAC. It is found that the NO_3^- ion forms an isosceles triangle in molten $LiNO_3$, $AgNO_3$ and $TlNO_3$, and a regular triangle in molten $NaNO_3$, KNO_3, $RbNO_3$ and $CsNO_3$.

1. Introduction

The structure of molten nitrates has been studied by many investigators using Raman scattering [1–7], infra-red absorption [8–10] and X-ray diffraction [11]. According to these studies the NO_3^- ion forms a regular triangle in these melts.

The structure of the NO_3^- ion is usually determined by Raman scattering and infra-red absorption experiments. These methods, however, cannot yield absolute values of the bond lengths in NO_3^- [12], but only the spatial symmetry of the ion. X-ray diffraction measurements, on the other hand, can give both the size and shape of the NO_3^- ion in molten nitrates [11], but conventional X-ray diffraction is not powerfull in the determination of the bond lengths and their fluctuations in NO_3^-, since in that method the maximum wave number is limited by relatively low values of Q ($=4\pi \sin\Theta/\lambda$, 2Θ: scattering angle, λ: wavelength), for example $17\,A^{-1}$ for MoKα-radiation, and the scattering amplitudes of the nitrogen and oxygen atoms are fairly small compared with those of the metal atoms in MNO_3.

In this work, the structure factors $S_m(Q)$ of molten monovalent metal nitrates are measured over a wide range of Q values up to $40\,A^{-1}$ by means of time-of-flight pulsed neutron diffraction [13] using epithermal neutrons generated from an electron LINAC, so as to obtain highly-resoluted structual information on the NO_3^- ion in the molten state.

2. Experimental

The time-of-flight pulsed neutron diffractometer [13, 14] installed at the Tohoku University 300 MeV electron LINAC was used to measured the total structure factor $S_m(Q)$ of molten nitrates. A schematic diagram of the diffractometer is shown in Figure 1. The essential features of the diffractometer are not different from those presented in a previous report [14], except for the arrangement of counters at backward-scattering angles.

In order to increase effectively the counting rates over the range of Q from 15 to $40\,A^{-1}$, a multi-counters time-focusing systems [15, 16] was adopted for the backward-scattering angles. The counters layout and instrumental parameters in the backward-scattering system are shown in Figure 2.

Neutrons scattered from a sample were simultaneously detected at four fixed scattering angles of $2\Theta = 5$, 15, 30 and 60°, and one variable backward-scattering angle located around $2\Theta = 145.3°$, using He-3 counters (Reuter Stokes, 10 atm. He-3, 1 inch diameter for $2\Theta = 5$, 15, 30 and 60° and 20 atm. He-3, 1 inch diameter for $2\Theta = 145.3°$).

The neutron counts were stored in a computer (OKITAC 4500), as a function of the time-of-flight of neutrons running definite path lengths, through ordinary electronic amplifiers and pulse height analysers. The flight path length for the incident neutrons is 4.359 m, while short path lengths are used for the sacttered neutrons, i. e. 1.50 m for the scattering angle $2\Theta = 5°$, 0.44 m for $2\Theta = 15°$, 0.42 m for $2\Theta = 30°$ and 60°, and 0.32 m for $2\Theta = 145.3°$.

Furthermore, the resolution widths available in the high Q region were much improved by using a variable channel width system ($2 \sim 16\,\mu$sec/channel) in the time analysing computer. The operating conditions of the LINAC and procedures of data processing are almost identical with those described fully in the previous paper [14].

The samples were sealed in vacuo in silica tubes with 0.3 mm wall thickness, 10 mm inner diameter and 70 mm length. Before sealing, all samples were dried at 120 to 150 °C in vacuo for 24 to 72 hours. During the measurements, the temperature of the

Reprint requests to Prof. Kenji Suzuki, The Research Institute for Iron, Steel and Other Metals, Tohoku University, 2-1-1 Katahira, *Sendai-980*, Japan.

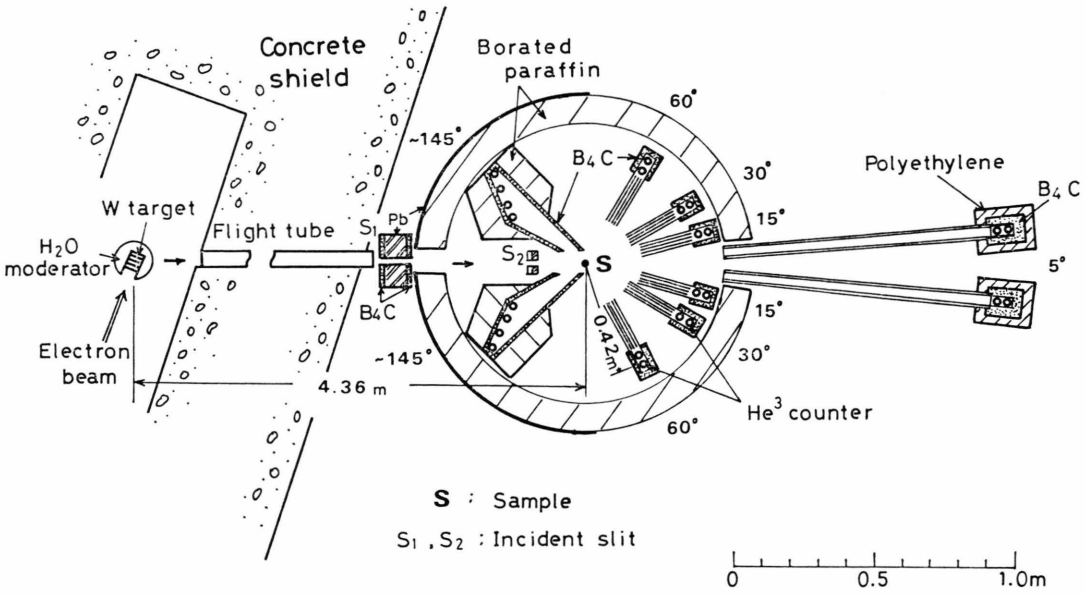

Fig. 1. Schematic diagram of the T—O—F pulsed neutron diffractometer installed at the Tohoku University 300 MeV electron LINAC.

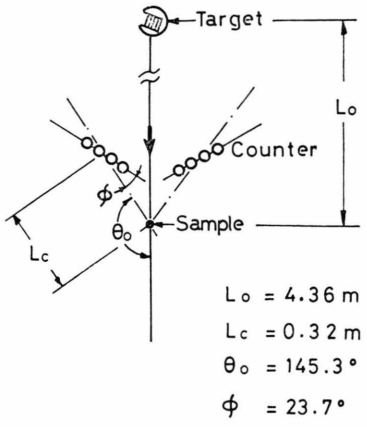

Fig. 2. Counters layout and instrumental parameters in the backward-scattering system.

liquid was kept, by an electric furnace[17], at 280, 340, 390, 350, 450, 260 and 250 °C for $LiNO_3$, $NaNO_3$, KNO_3, $RbNO_3$, $CsNO_3$, $AgNO_3$ and $TlNO_3$, respectively. These temperatures were held with an accuracy of within ±10 °C.

Besides the sample runs, measurements were carried out with empty silica tubes, background and a vanadium rod with the same dimensions in diameter and length as the sample. Details of the corrections for absorption, multiple scattering, silica tubes, etc., and the deduction of structure factors have been described in previous papers[14, 18].

3. Results

3.1. Structure Factors

Figure 3 shows the structure factors $S_m(Q)$ obtained experimentally. Here $S_m(Q)$ is defined as

$$S_m(Q) \to \sum_n b_n^2 / (\sum_n b_n)^2, \quad \text{when} \quad Q \to \infty, \quad (1)$$

where b_n is the mean coherent scattering amplitude of nucleus n and the sum over n is extended to all nuclei in the chemical formula MNO_3.

Large differences are found in $S_m(Q)$ in the range of $Q < 5\ A^{-1}$, depending on the cationic species. In this region there must be contained a lot of information about inter-ionic correlations of $M^+ - M^+$, $M^+ - NO_3^-$ and $NO_3^- - NO_3^-$ pairs. On the other hand, the $S_m(Q)$ in the high Q region clearly show that there the oscillatory behaviour is very similar.

3.2. Radial Distribution Functions

Pair correlation functions $g(r)$ of molten nitrates are obtained as Fourier transforms of $S_m(Q)$ as follows,

$$4\pi\varrho_0\{g(r)-1\} = \frac{2}{\pi}\int_0^{Q_{max}} Q\, m \cdot \left\{S_m(Q) - \sum_n b_n^2 \Big/ \Big(\sum_n b_n\Big)^2\right\} \sin(Q\cdot r)\, dQ, \quad (2)$$

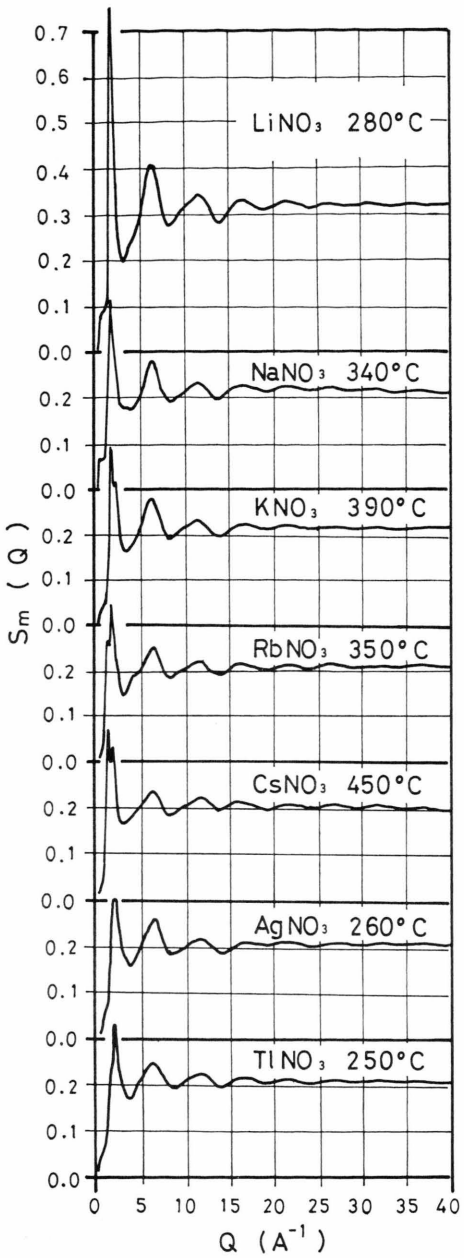

Fig. 3. Structure factors of molten $LiNO_3$, $NaNO_3$, KNO_3, $RbNO_3$, $CsNO_3$, $AgNO_3$ and $TlNO_3$.

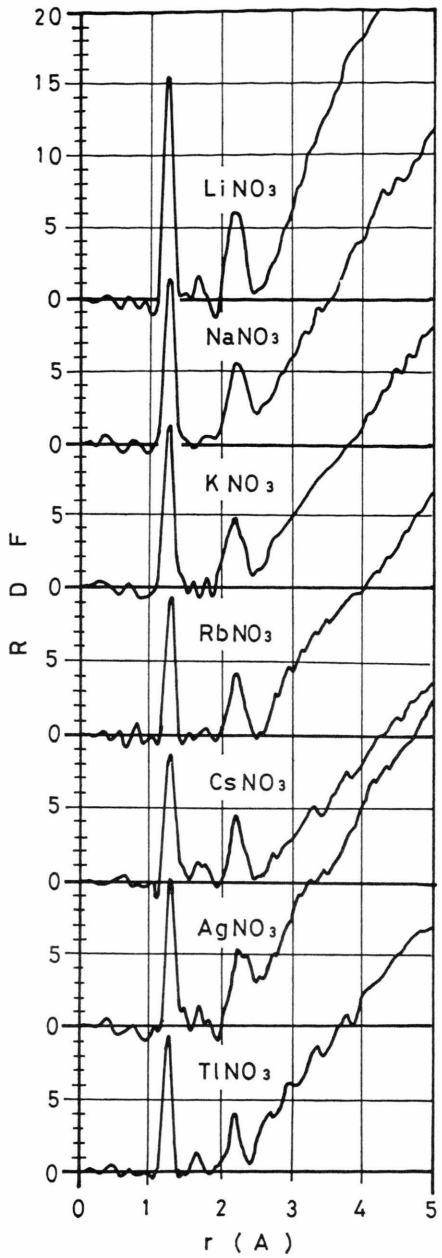

Fig. 4. Radial distribution functions (RDF) of molten $LiNO_3$, $NaNO_3$, KNO_3, $RbNO_3$, $CsNO_3$, $AgNO_3$ and $TlNO_3$.

were ϱ_0 is the atomic average number density and m is the number of atoms in the chemical formula MNO_3. Radial distribution functions RDF defined as $4\pi r^2 \varrho_0 g(r)$ are shown in Figure 4. The numerical integration of Eq. (2) was truncated at $Q_{max} = 38\ A^{-1}$ for all RDF's. RDF's of molten nitrates have generally a sharp peak at $r = 1.25$ to 1.27 A, which corresponds to the N – O bond. The second peak near $r = 2.2$ A is suggested to display the O – O separation in the NO_3^- ion. From the areas under the first and second peaks in the RDF's it follows that there are three N – O pairs and three O – O pairs in an NO_3^- ion.

4. Discussion

4.1. Second Peak Profiles in RDF's

If the structure of NO_3^- in molten nitrates is assumed to be a regular triangle having a nitrogen atom at its centre (Figure 5), the three $O-O$ side lengths of the regular triangle must be $r_{OO} = 2.17$ A, because the bond length between nitrogen and oxygen is approximately $r_{NO} = 1.25$ A as indicated from the RDF's in Figure 4.

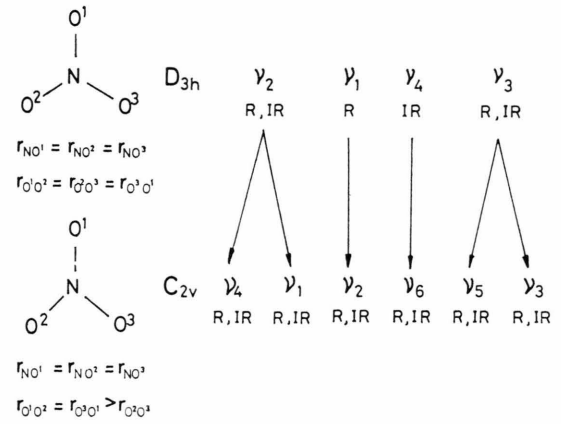

Fig. 5. Regular and isosceles triangle models for the NO^{3-} ion in molten nitrates and the correlation of fundamental modes of vibration between D_{3h} and C_{2v} symmetries [19].

In Figure 6, Gaussian profiles having their centres at 2.17 A are superimposed on the second peaks of the RDF's of molten $LiNO_3$, $NaNO_3$ and $RbNO_3$. Figure 6 clearly shows that the Gaussian profile coincides well with the whole second peak of $RbNO_3$ and the left hand side of the second peak of $NaNO_3$, while for $LiNO_3$ the centre of the second peak is shifted towards $r > 2.17$ A.

The $O-O$ distance in NO_3^- is different from the Rb^+-O and Rb^+-N distances in the RDF of molten $RbNO_3$, because Rb^+ has a diameter which is considerably larger than the $O-O$ distance. On the other hand, an overlapping happens between the $O-O$ distance and the Na^+-O or Na^+-N distances, since the Na^+ ion is smaller. In molten $NaNO_3$ and $RbNO_3$, the NO_3^- ion can thus be concluded to be a regular triangle. The same holds for molten KNO_3 and $CsNO_3$, respectively, resulting again in the regular triangle form of NO_3^-.

The second peak of $LiNO_3$ shown in Fig. 6 cannot be understood in terms of a regular triangle but leads to the assumption that it consists of two Gaussian profiles having their centres at 2.09 and 2.21 A respectively, where the ratio of the areas under the Gaussian profiles it 1 to 2 as shown in Figure 7. This means that NO_3^- in molten $LiNO_3$ is deformed into an isosceles triangle (Figure 5). A similar discussion leads to the conclusion that also in molten $AgNO_3$ and $TlNO_3$ the NO_3^- ions are isosceles triangles.

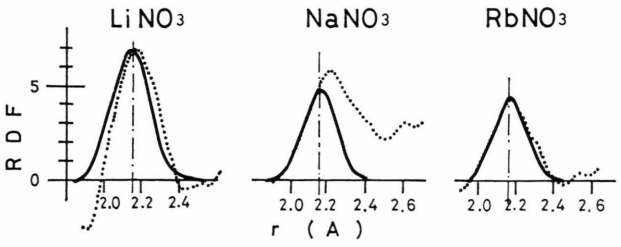

Fig. 6. Gaussian profiles having their centre at 2.17 A (full lines) and the second peaks of the RDF's of molten $LiNO_3$, $NaNO_3$ and $RbNO_3$ (dotted lines).

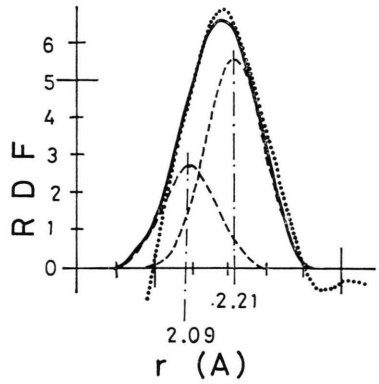

Fig. 7. Gaussian profiles having their centres at 2.09 and 2.21 A, where the ratio of areas under the Gaussian profiles is 1 to 2 (broken lines), profile of the sum of these two Gaussians (full line) and the second peak of RDF of molten $LiNO_3$ (dotted line).

4.2. $S_m(Q)$ in the High Q Region

The structure factor $S_m(Q)$ of molten nitrates can be divided into contributions from intra-NO_3^- and inter-ionic correlations as follows,

$$S_m(Q) = \left(\sum_n b_n\right)^{-2} \{F_{NO_3^-}(Q) + S_{inter}(Q)\}, \quad (3)$$

where $F_{NO_3^-}(Q)$ is the form factor for a single NO_3^- ion and $S_{inter}(Q)$ is the sum of the structure factors of the M^+-M^+, $M^+-NO_3^-$ and $NO_3^--NO_3^-$ inter-ionic correlations.

When Q is increased, the oscillatory behaviour of $S_m(Q)$ asymptotically approaches $F_{NO_3^-}(Q)$,

$$S_m(Q) \rightarrow \left(\sum_n b_n\right)^{-2} \{F_{NO_3^-}(Q) + b_{M^+}^2\}, \quad \text{when } Q \rightarrow \infty, \qquad (4)$$

because the correlation in $S_{inter}(Q)$ diminish away to become $b_{M^+}^2$ in the high Q region since the $M^+ - M^+$, $M^+ - NO_3^-$ and $NO_3^- - NO_3^-$ inter-ionic correlations extend over a long range and are weak compared with the intra-NO_3^- correlations. Therefore the exact form of a single NO_3^- ion in the molten state can directly be estimated from the behaviour of $S_m(Q)$ in the high Q region.

If all atomic vibrations in NO_3^- are assumed to be independent of one another, the ionic form factor $F_{NO_3^-}$ can be written as

$$F_{NO_3^-}(Q) = F_N(Q) + F_0(Q) + F_{NO}(Q) + F_{OO}(Q), \qquad (5)$$

where $F_N(Q) = b_N^2$, $F_O(Q) = 3\,b_O^2$,

$$F_{NO}(Q) = 6\,b_N\,b_O \cdot \frac{\sin(Q \cdot r_{NO})}{Q \cdot r_{NO}} \cdot \exp\left(-\frac{\langle \Delta_{NO}^2 \rangle}{2} \cdot Q^2\right)$$

and

$$F_{OO}(Q) = \begin{cases} 6\,b_O \cdot \dfrac{\sin(Q \cdot r_{OO})}{Q \cdot r_{OO}} \cdot \exp\left(-\dfrac{\langle \Delta_{OO}^2 \rangle}{2} \cdot Q^2\right) \\ \text{for regular triangle form,} \\ 2\,b_O \cdot \dfrac{\sin(Q \cdot r_{OO}^{I})}{Q \cdot r_{OO}^{I}} \cdot \exp\left(-\dfrac{\langle (\Delta_{OO}^{I})^2 \rangle}{2} \cdot Q^2\right) \\ + 4\,b_O \cdot \dfrac{\sin(Q \cdot r_{OO}^{II})}{Q \cdot r_{OO}^{II}} \cdot \exp\left(-\dfrac{\langle (\Delta_{OO}^{II})^2 \rangle}{2} \cdot Q^2\right) \\ \text{for the isosceles triangle form.} \end{cases}$$

In order to make a clear comparison, the discussion shall be focused on the O – O correlations. Figure 8 shows comparisons between

$$S_m(Q) - \left(\sum_n b_n\right)^{-2} \cdot \{F_N(Q) + F_O(Q) + F_{NO}(Q) + b_M^2 + \}$$

and

$$\left(\sum_n b_n\right)^{-2} \cdot F_{OO}(Q)$$

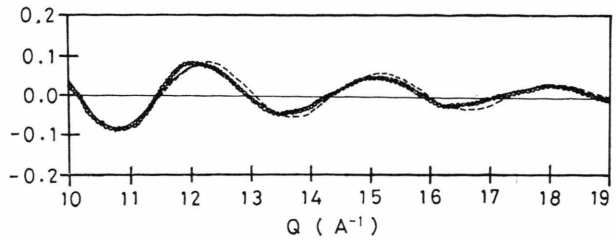

Fig. 8. Form factors $(\sum_n b_n)^{-2} F_{OO}(Q)$ of the O–O distance in the NO_3^- ion in molten $LiNO_3$ calculated by means of the regular triangle model (broken line) and the isosceles triangle model (full line) and $S_m(Q) - (\sum_n b_n)^{-2} \{F_N(Q) + F_O(Q) + F_{NO}(Q) + b_{Li^+}^2\}$ (blank circles).

for both the regular and isosceles triangle models of the NO_3^- ion in molten $LiNO_3$ over the range 10 to 19 A^{-1}. A good agreement is found between the observation and the isosceles triangle model. The N – O bond lengths, O – O distances and their fluctuations obtained by least squares fittings are summarized in Table 1.

4.3. Comparison with Vibrational Spectroscopic Experiments

The D_{3h} symmetry of a free NO_3^- ion having the form of a regular triangle dictates that it must have

	r_{NO} (A)	$\langle \Delta_{NO}^2 \rangle / 2$ (A^2)	r_{OO} (A)	$\langle \Delta_{OO}^2 \rangle / 2$ (A^2)
$LiNO_3$	1.26 ±0.001	0.0014 ±0.0001	2.09 2.21 ±0.004	0.0025 ±0.0003
$NaNO_3$	1.25 ±0.001	0.0015 ±0.0001	2.17 ±0.005	0.0031 ±0.0005
KNO_3	1.26 ±0.001	0.0017 ±0.0001	2.17 ±0.005	0.0027 ±0.0004
$RbNO_3$	1.25 ±0.001	0.0010 ±0.0001	2.17 ±0.004	0.0018 ±0.0004
$CsNO_3$	1.26 ±0.002	0.0014 ±0.0002	2.18 ±0.006	0.0026 ±0.0009
$AgNO_3$	1.27 ±0.002	0.0016 ±0.0001	2.10 2.22 ±0.005	0.0025 ±0.0005
$TlNO_3$	1.25 ±0.001	0.0011 ±0.0001	2.14 2.20 ±0.005	0.0031 ±0.0005

Table 1. N – O and O – O pair distances in the NO_3^- ion in molten monovalent metal nitrates

four fundamental modes [19] as shown in Fig. 5, where *R* and IR refer to Raman active and infra-red active vibrational modes, respectively. When NO_3^- is an isosceles triangle, then the C_{2v} symmetry holds [19].

The correlation of the fundamental modes of vibration between the D_{3h} and C_{2v} symmetries [19] is shown in Figure 5. Features characteristic of the C_{2v} splitting pattern have been observed [2, 4, 6, 9, 10, 20] for molten $LiNO_3$, $AgNO_3$ and $TlNO_3$. These spectroscopic data are thus consistent with the results of this work. Studies of the structure of $M^+ - NO_3^-$ pairs would be interesting and necessary to confirm the isosceles triangle model of NO_3^- in some molten nitrates. This will be the subject of a separate report.

5. Conclusion

The structure factors of molten monovalent metal nitrates were measured over Q ranges from 0.1 to 40 A^{-1} by time-of-flight pulsed neutron diffraction using hot neutrons produced from an electron LINAC. The size and shape of the NO_3^- ions were investigated by means of highly-resoluted radial distribution functions and structure factors in the high Q region. It is concluded that the NO_3^- ion is a regular triangle in molten $NaNO_3$, KNO_3, $RbNO_3$ and $CsNO_3$, and an isosceles triangle in molten $LiNO_3$, $AgNO_3$ and $TlNO_3$. These results are consistent with the observations of vibrational spectroscopy.

Acknowledgements

The authors would like to thank Dr. Misawa for helpful discussions and the members of the Nuclear Science Laboratory, Tohoku University, for the operation of the electron LINAC.

[1] P. Grassman, Z. Phys. **77,** 616 [1932].
[2] W. Bus, Z. Phys. Chem. (Frankfurt) **10,** 1 [1957].
[3] Y. Doucet and J. Vallier, Comp. Rend. **35,** 739 [1966].
[4] G. J. Janz and D. W. James, J. Chem. Phys. **35,** 739 [1961].
[5] G. E. Walrafen and D. E. Irish, J. Chem. Phys. **40,** 911 [1964].
[6] G. J. Janz, T. R. Kozlowski, and S. C. Wait, Jr., J. Chem. Phys. **39,** 1809 [1963].
[7] E. F. Gross and V. A. Koksva, Acad. Nauk. SSSR Pamyati S. I. Vavilova, 231 [1952].
[8] J. Greenberg and L. J. Hallgen, J. Chem. Phys. **33,** 900 [1960].
[9] J. K. Wilmschurst and S. S. Senderoff, J. Chem. Phys. **35,** 1078 [1961].
[10] J. P. Devlin, K. Williamson, and G. Austin, J. Chem. Phys. **44,** 2203 [1966].
[11] H. Ohono and K. Furukawa, J. Chem. Soc. Faraday Trans., to be published.
[12] G. J. Janz and Y. Mikawa, J. Molecular Spect. **1,** 92 [1960].
[13] K. Suzuki, Berichte Bunsen-Gesell. Phys. Chem. **80,** 689 [1976].
[14] K. Suzuki, M. Misawa, K. Kai, and N. Watanabe, Nucl. Inst. Method, to be published.
[15] R. N. Sinclair, D. A. G. Johnson, D. C. Dore, J. H. Clarke, and A. C. Wright, Nucl. Inst. Method **117,** 445 [1974].
[16] J. G. Powles, Mol. Phys. **26,** 1325 [1973].
[17] K. Suzuki, M. Misawa, and Y. Fukushima, Trans. Japan Inst. Metals **16,** 297 [1975].
[18] M. Misawa, K. Kai, K. Suzuki, and S. Takeuchi, Res. Report Lab. Nucl. Sci., Tohoku Univ. **5** [2], 73 [1972].
[19] R. E. Hester, Advances in Molten Salt Chemistry, Vol. 1, edited by J. Braunstein, G. Mamanotov, and G. P. Smith, Plenum Press, New York 1971, P 36.
[20] J. R. Ferraro and A. Walker, J. Chem. Phys. **42,** 1273 [1965].